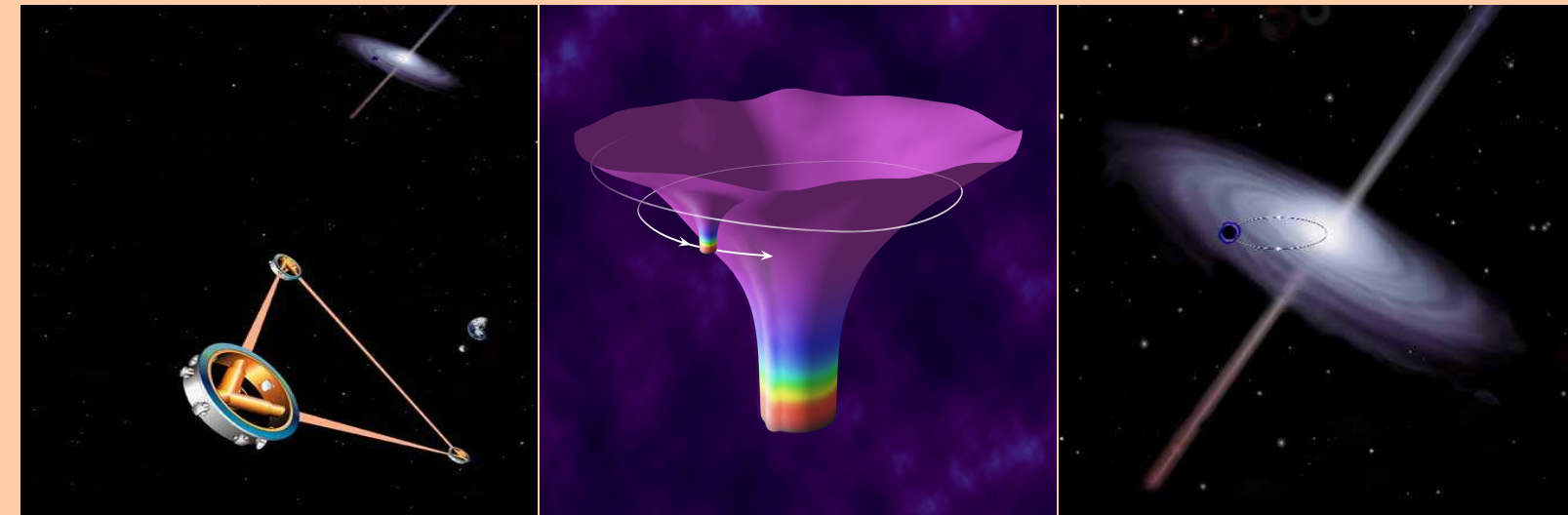


Abstract: Extreme-Mass-Ratio Binary systems in the inspiral phase (EMRIs) are a primary source of gravitational waves for the NASA/ESA Laser Interferometric Space Antenna (LISA). Data analysis techniques for detection and extraction of physical information will require an *a priori* theoretical knowledge of the waveforms with a certain precision. In this poster we report the results of numerical simulations in the Time Domain of EMRIs. These computations are based on Finite Element Methods and their final goal is to achieve simulations accurate enough for estimating the radiation reaction effects in the gravitational waveforms.

Main Motivation

EMRIs consist of a stellar-type object, with mass $m \sim 1 - 10^2 M_\odot$, orbiting around a Super-Massive Black Hole (SMBH), with mass $M_\bullet \sim 10^5 - 10^8 M_\odot$. The range of mass ratios is: $\mu = m/M_\bullet \sim 10^{-3} - 10^{-8}$.



Typically, EMRIs spend around $10^5 - 10^6$ cycles inside the LISA band during the last year before plunge. Although they circularize due to GW emission, they have substantial eccentricities. Data analysis techniques for detection and extraction of physical information require a theoretical knowledge of the waveforms with accuracy: $\delta\varphi_{gw} \sim 1$ over ~ 3 weeks for detection; $\delta\varphi_{gw} \sim 1$ over ~ 1 yr for extraction of physical information.

The Computational Challenge

- The framework to describe EMRIs is relativistic perturbation theory and the steps to follow are: (i) To compute the perturbations created by the stellar-type object in the space-time geometry of the SMBH. (ii) To estimate how these perturbations affect the orbital motion of the stellar-type object (the radiation reaction effects). (iii) To compute the waveforms of generated in the inspiral.

- Numerical methods are needed in order to solve the partial differential equations involved. Since many of the relevant EMRIs will have high eccentricities, Time-Domain methods seem more appropriate than Frequency-Domain ones.

- The choice of numerical techniques should take into account the following points:

- We have to deal with different spatial (and temporal) scales \rightarrow Grid adaptivity.
- We have to deal with singular source terms associated with the energy-momentum distribution of the stellar-type object.
- The computations require high accuracy.
- Time-domain simulations of EMRIs may have to face stability problems and the appearance of spurious high-frequency modes.

Our Computational Techniques

- Our choice is: Finite Element methods (FEMs) for spatial discretizations and Finite Differences methods (linked to the FEM) for the time discretization.

- The main features of FEMs are: (i) Can deal with *Computational domains* of arbitrary geometries. (ii) Incorporate naturally the *Boundary Conditions* of the problem. (iii) Provide systematic ways of dealing with singular sources like the ones that we encounter in the description of EMRIs. (iv) Provide grid adaptivity in a natural manner. (v) There is a great variety of computational infrastructure available for FEMs.

A Toy Model in Scalar Gravity

As a testbed of the numerical techniques we have studied a toy model that contains the main ingredients of actual EMRIs:

- The SMBH is described by the Schwarzschild solution [in scalar gravity the metric is *not* dynamic] and the stellar-type object is described as a particle following a trajectory $\mathbf{z}(t)$ around the SMBH.
- The dynamical gravitational field is described by a scalar field Φ satisfying the following wave-like equation:

$$g_{\text{Sch}}^{\mu\nu} \nabla_\mu \nabla_\nu \Phi = 4\pi e^\Phi \rho, \quad \rho = \frac{m}{u^t \sqrt{-g}} \delta[\mathbf{x} - \mathbf{z}(t)]$$

- The trajectory of the stellar-mass object is determined by the following equations of motion:

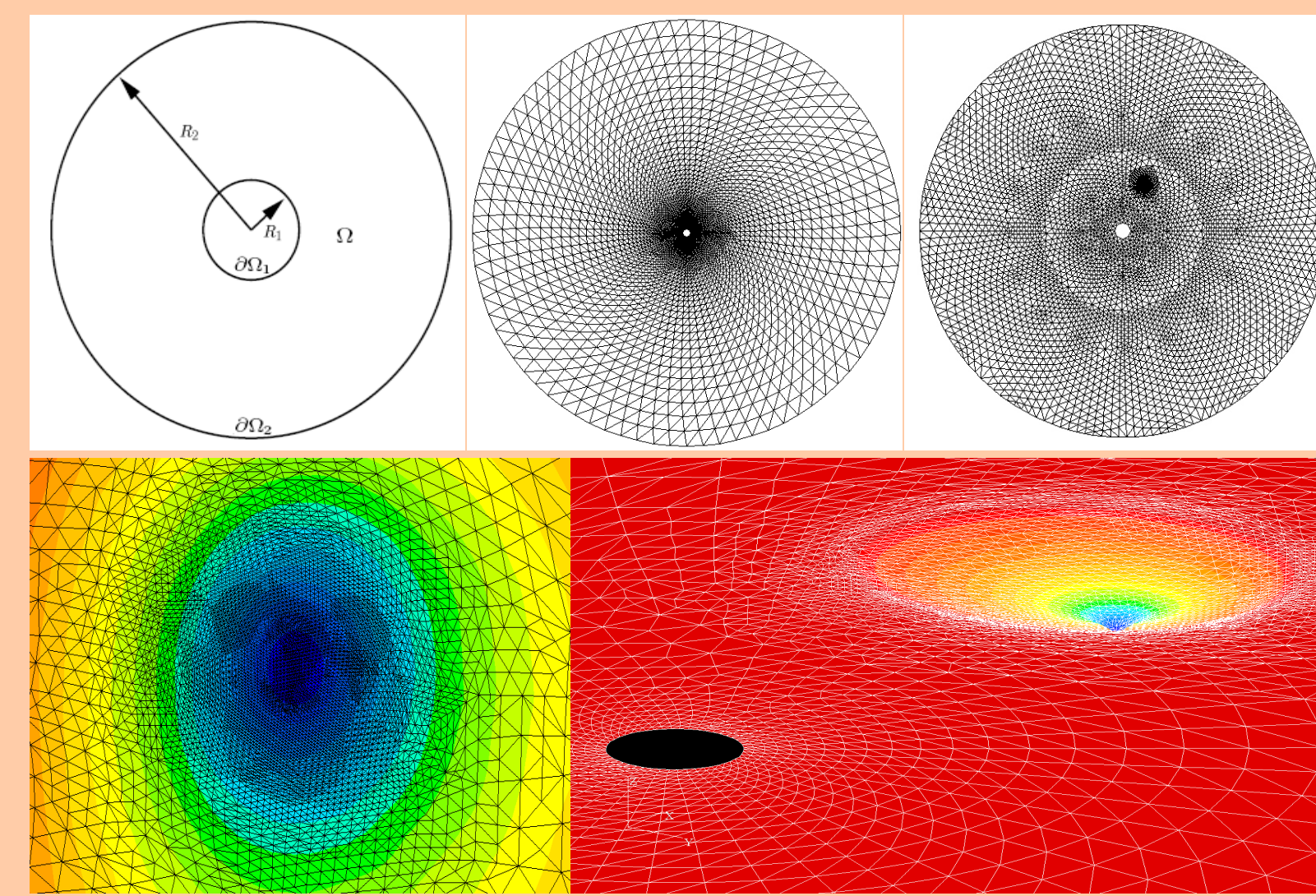
$$\dot{\mathbf{z}}(t) = \mathbf{v}(t), \quad \dot{\mathbf{v}}(t) = \mathbf{f}_{\text{SMBH}} + \mathbf{f}_\Phi$$

A Toy Model in Scalar Gravity

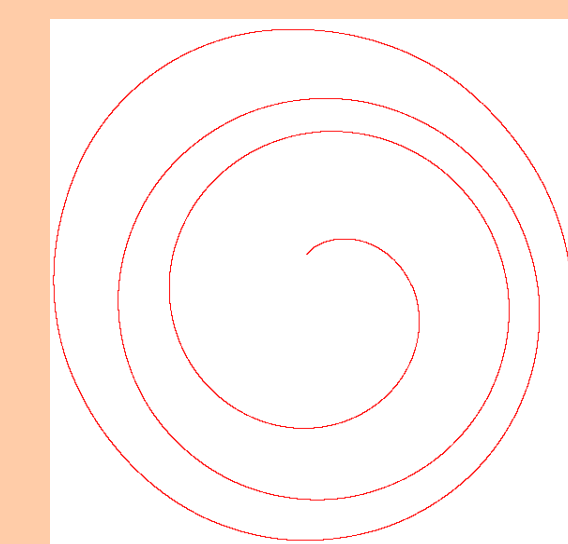
The first force, \mathbf{f}_{SMBH} , describes the force due to the presence of the SMBH and is a *conservative* force term in the sense that it does not produce any loss of energy or angular momentum. The second force, \mathbf{f}_Φ , is due to the stellar object own gravitational field (*self-force* term) and is a dissipative force term in the sense that it makes the orbit around the Black Hole to shrink as energy is carried away from the system in the form of Gravitational Waves (radiation reaction mechanism).

Toy Model Simulations

- Domain discretization and Adaptivity:

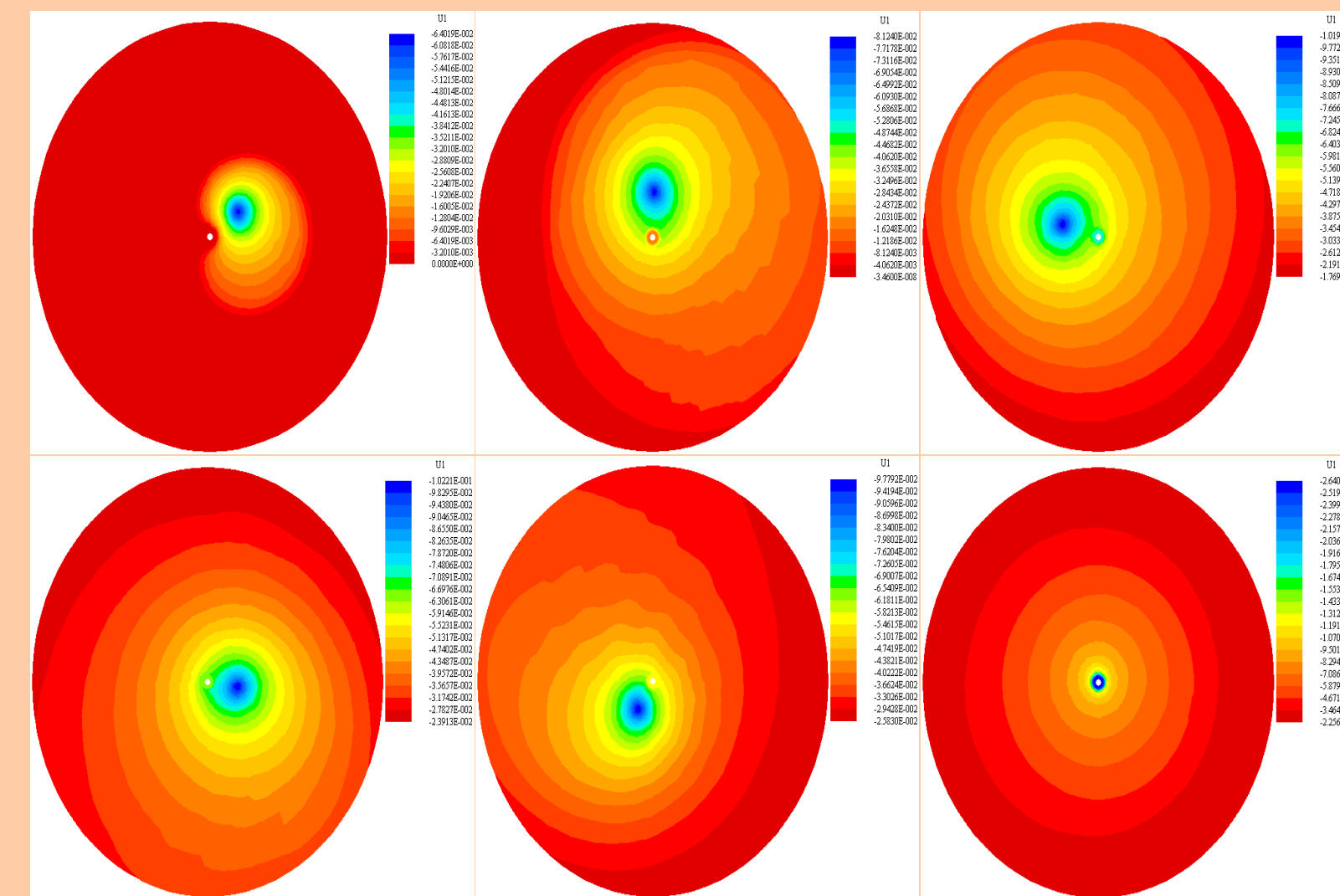


- Trajectory:

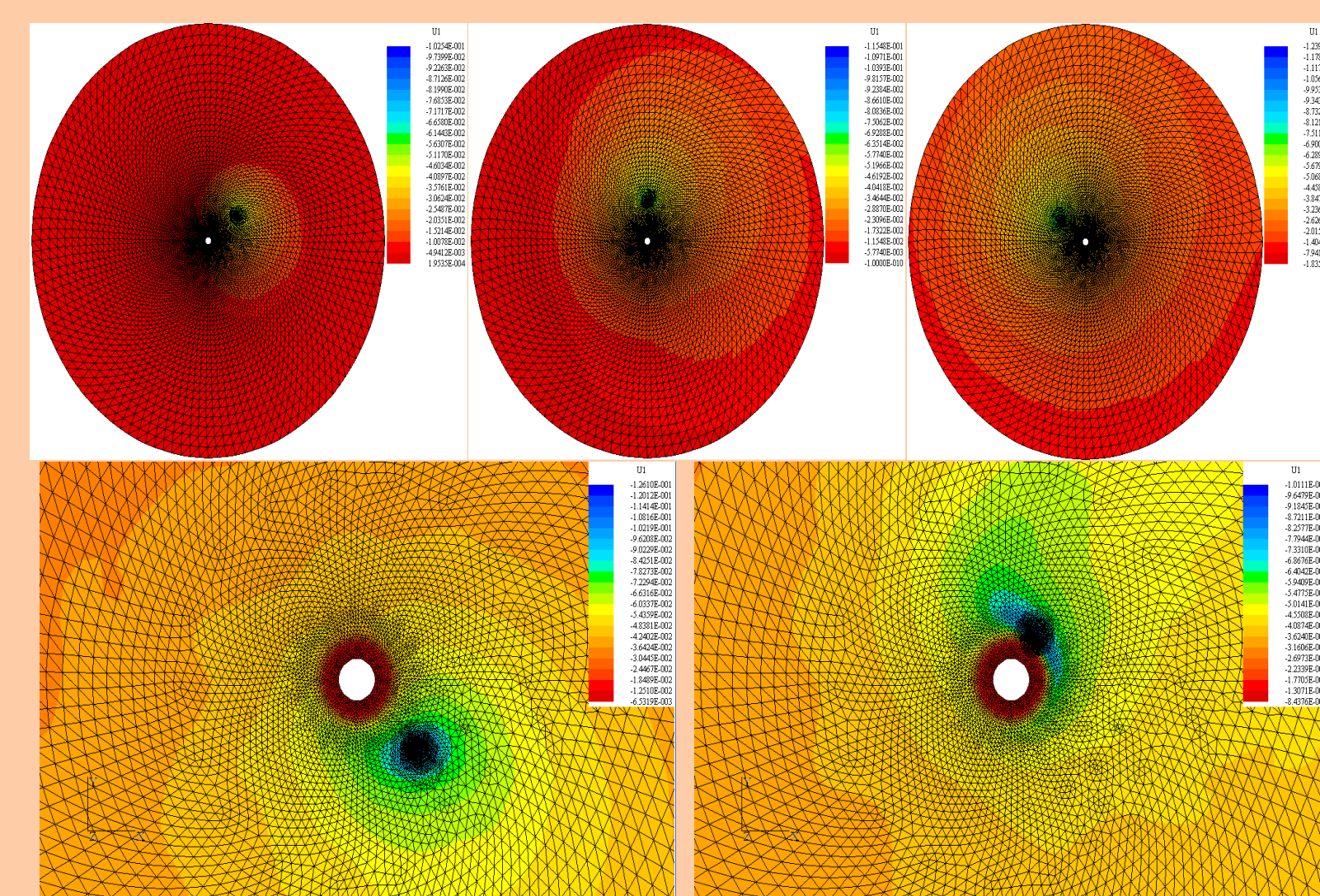


The system stellar mass-object plus scalar gravitational field has a CONSERVATION LAW which tells us that *the difference in energy from two different times must be equal to the energy radiated away from the system in Gravitational Waves (both to infinity and into the horizon).*

- Evolutions WITHOUT Adaptivity (the particle is described as a Gaussian packet): For a mesh of $\sim 10^4$ triangles we observe that the width of the Gaussian cannot be smaller than $\sim 1M$.



- Evolutions WITH Adaptivity: Using a similar number of triangles ($\sim 1.1 \times 10^4$) we can reduce the Gaussian width in one order of magnitude, i.e. to $\sim 0.1M$.



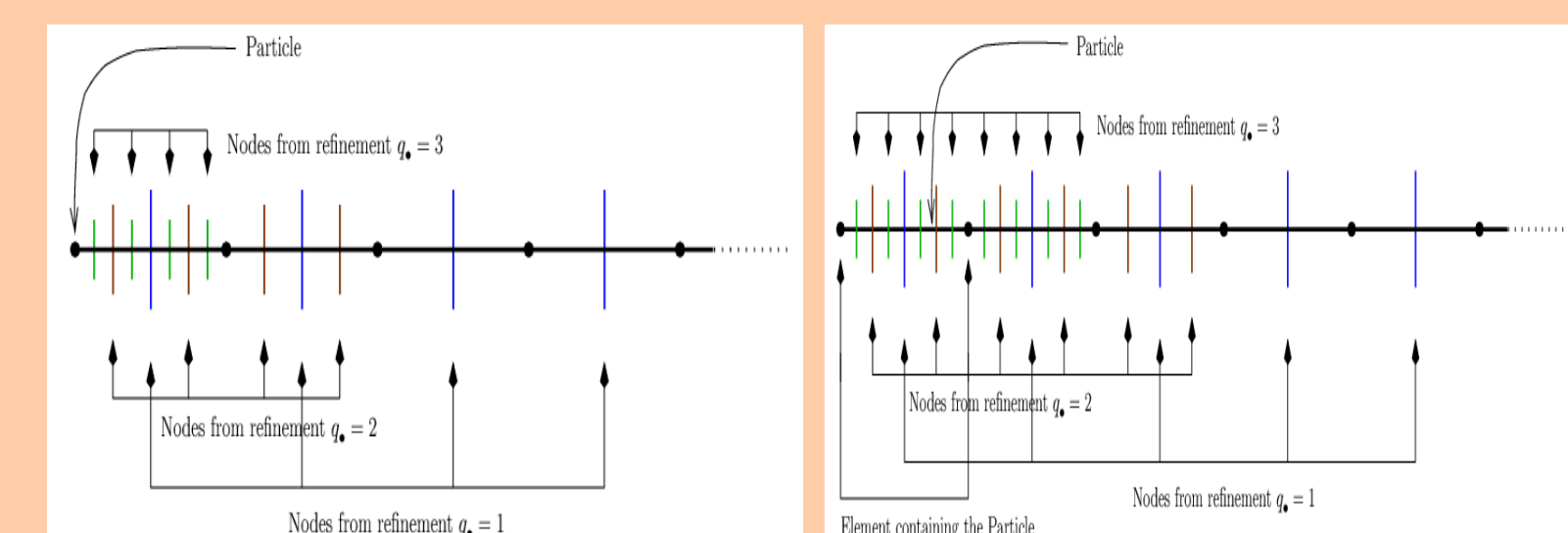
Simulations in the Regge-Wheeler gauge

- We have used FEMs to relativistic perturbations created by a stellar-type object orbiting a non-rotating SMBH. In the Regge-Wheeler gauge, the perturbations are described by wave-like master equations:

$$\left[-\partial_t^2 + \partial_r^2 - V(r)\right] \Psi^{\ell m} = S^{\ell m}$$

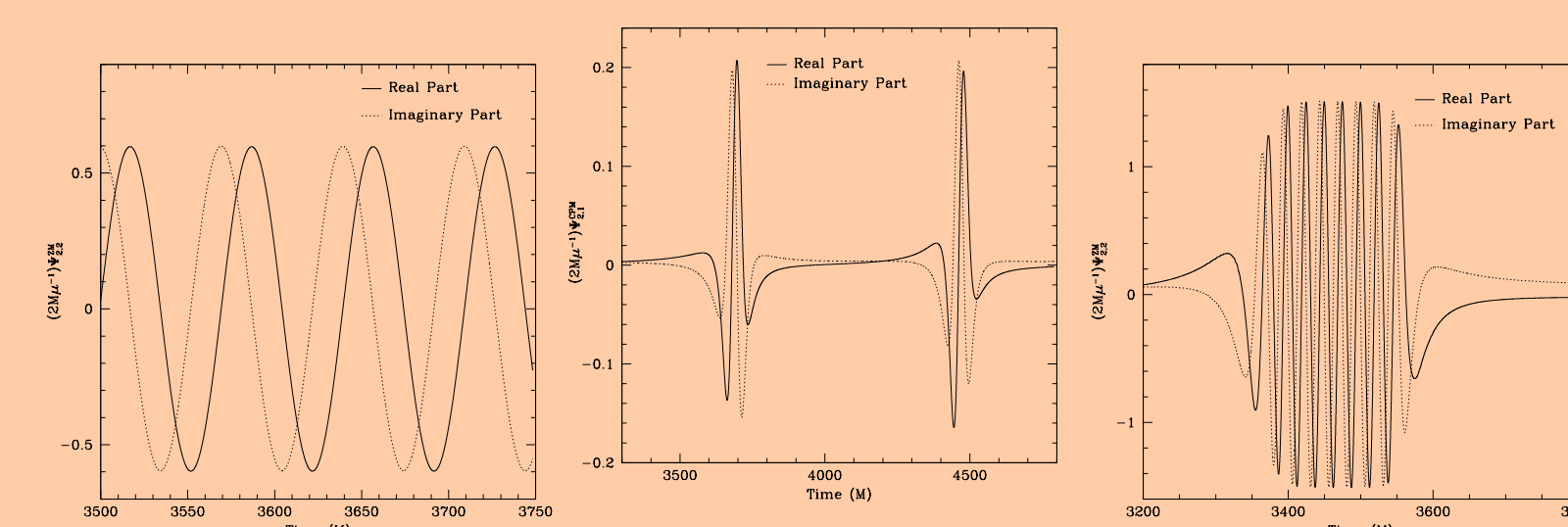
$$S^{\ell m}(t, r) = F(t, r) \delta[r - r_p(t)] + G(t, r) \delta'[r - r_p(t)]$$

- We use 1D grids concentrating elements around the stellar-type object to resolve properly the singular source terms associated with it:



Numerical Results

- Waveforms:



Circular orbits Orbits with $e = 0.76$ Zoom-Whirl orbits

- Comparison with Frequency Domain calculations: Circular orbits with $p = 7.9456$ [Poisson, PRD **52**, 5719 (1995)].

(ℓ, m)	E_{TD}^∞	L_{TD}^∞	E_{FD}^∞	L_{FD}^∞
(2,1)	$8.1662 \cdot 10^{-7}$	$1.8289 \cdot 10^{-5}$	$8.1633 \cdot 10^{-7}$ [0.04%]	$1.8283 \cdot 10^{-5}$ [0.04%]
(2,2)	$1.7064 \cdot 10^{-4}$	$3.8219 \cdot 10^{-3}$	$1.7063 \cdot 10^{-4}$ [0.006%]	$3.8215 \cdot 10^{-3}$ [0.01%]
(3,1)	$2.1732 \cdot 10^{-9}$	$4.8675 \cdot 10^{-8}$	$2.1731 \cdot 10^{-9}$ [0.005%]	$4.8670 \cdot 10^{-8}$ [0.01%]
(3,2)	$2.5204 \cdot 10^{-7}$	$5.6450 \cdot 10^{-6}$	$2.5199 \cdot 10^{-7}$ [0.02%]	$5.6439 \cdot 10^{-6}$ [0.02%]
(3,3)	$2.5475 \cdot 10^{-5}$	$5.7057 \cdot 10^{-4}$	$2.5471 \cdot 10^{-5}$ [0.02%]	$5.7048 \cdot 10^{-4}$ [0.02%]
(4,1)	$8.4055 \cdot 10^{-13}$	$1.8825 \cdot 10^{-11}$	$8.3956 \cdot 10^{-13}$ [0.12%]	$1.8803 \cdot 10^{-11}$ [0.12%]
(4,2)	$2.5099 \cdot 10^{-9}$	$5.6215 \cdot 10^{-8}$	$2.5091 \cdot 10^{-9}$ [0.04%]	$5.6195 \cdot 10^{-8}$ [0.04%]
(4,3)	$5.7765 \cdot 10^{-8}$	$1.2937 \cdot 10^{-6}$	$5.7751 \cdot 10^{-8}$ [0.03%]	$1.2934 \cdot 10^{-6}$ [0.03%]
(4,4)	$4.7270 \cdot 10^{-6}$	$1.0586 \cdot 10^{-4}$	$4.7256 \cdot 10^{-6}$ [0.03%]	$1.0584 \cdot 10^{-4}$ [0.02%]
(5,1)	$1.2607 \cdot 10^{-15}$	$2.8237 \cdot 10^{-14}$	$1.2594 \cdot 10^{-15}$ [0.1%]	$2.8206 \cdot 10^{-14}$ [0.1%]
(5,2)	$2.7909 \cdot 10^{-12}$	$6.2509 \cdot 10^{-11}$	$2.7896 \cdot 10^{-12}$ [0.05%]	$6.2479 \cdot 10^{-11}$ [0.05%]
(5,3)	$1.0936 \cdot 10^{-9}$	$2.4494 \cdot 10^{-8}$	$1.0933 \cdot 10^{-9}$ [0.03%]	$2.4486 \cdot 10^{-8}$ [0.04%]
(5,4)	$1.2329 \cdot 10^{-8}$	$2.7613 \cdot 10^{-7}$	$1.2324 \cdot 10^{-8}$ [0.04%]	$2.7603 \cdot 10^{-7}$ [0.04%]
(5,5)	$9.4616 \cdot 10^{-7}$	$2.1190 \cdot 10^{-5}$	$9.4563 \cdot 10^{-7}$ [0.06%]	$2.1179 \cdot 10^{-5}$ [0.06%]
Total	$2.0293 \cdot 10^{-4}$	$4.5451 \cdot 10^{-3}$	$2.0292 \cdot 10^{-4}$ [0.005%]	$4.5446 \cdot 10^{-3}$ [0.02%]

Elliptic orbits with (A) $(p, e) = (7.50478, 0.188917)$; (B) $(p, e) = (8.75455, 0.764124)$ [Cutler, Kennefick, and Poisson, PRD **50**, 3816 (1995)]

Orbit	$\langle \dot{E}^\infty \rangle$ (TD)	$\langle L^\infty \rangle$ (TD)	$\langle \dot{E}^\infty \rangle$ (FD)	$\langle L^\infty \rangle$ (FD)
A	$3.1672 \cdot 10^{-4}$	$5.9636 \cdot 10^{-3}$	$3.1680 \cdot 10^{-4}$ [0.03%]	$5.9656 \cdot 10^{-3}$ [0.04%]
B	$2.1004 \cdot 10^{-4}$	$2.7505 \cdot 10^{-3}$	$2.1008 \cdot 10^{-4}$ [0.02%]	$2.7503 \cdot 10^{-3}$ [0.01%]

Simulations in the Lorentz gauge

- Computations in the Regge-Wheeler gauge are sufficient to simulate an EMRI via the *adiabatic* approximation. However, if we want to include Radiation Reaction effects via self-force calculations, the following issues appear in the RW gauge:

- Some metric perturbations are singular (at the particle location) in the RW gauge.
- The *mode-sum scheme* for subtracting the singular piece of the self-force is formulated in the Lorentz gauge and the gauge transformation is singular.
- The singularities in the source terms of the evolution equations in the RW gauge are stronger (less differentiability of the solutions) than in the Lorentz gauge.

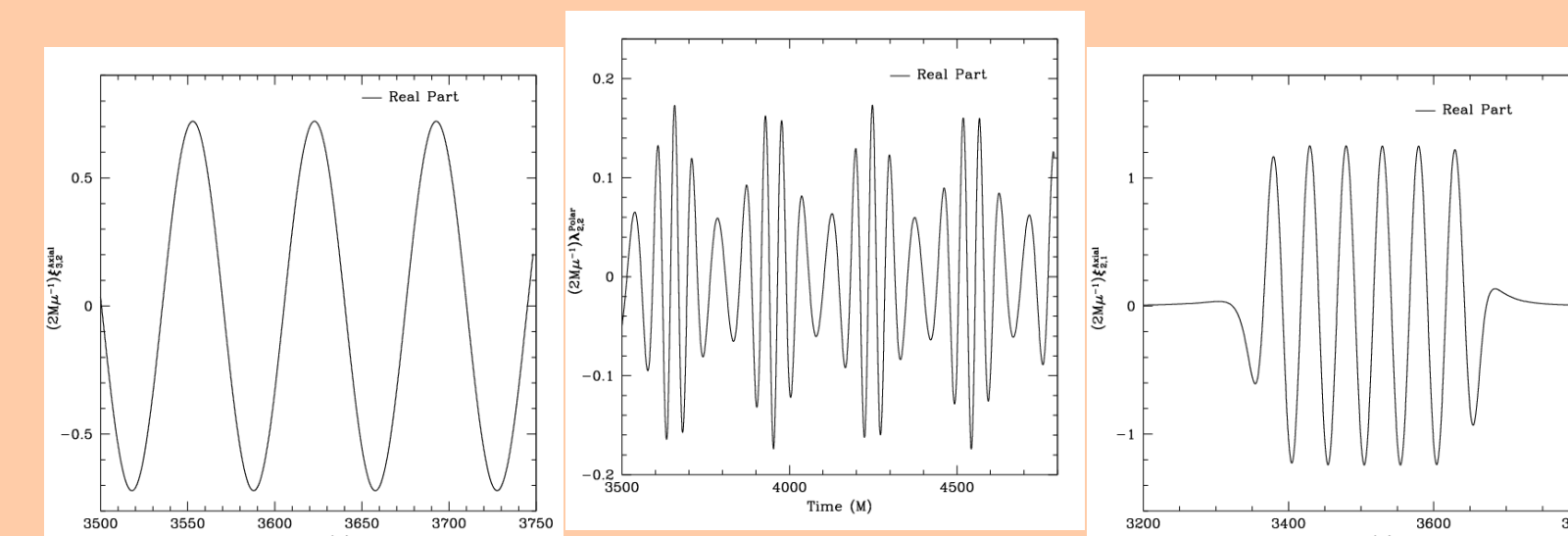
- See [Barack and Lousto, PRD **72**, 104026 (2005)] for a detailed list of advantages of working in the Lorentz gauge.

- These are much more complicated calculations since they involve many more variables and the system of equations is coupled and constrained. The form of the equations to solve is:

$$\Phi^\mu = \varphi_{,\nu}^{\mu\nu} = 0, \quad \varphi_{\mu\nu} = h_{\mu\nu} - \frac{1}{2} h g_{\mu\nu}^{\text{Sch}}$$

$$\varphi_{\mu\nu;\rho}^{\rho} + 2R_{\mu\nu}^{\text{Sch}\rho\sigma} \varphi_{\rho\sigma} = -16\pi m \int \frac{d\tau}{\sqrt{-g}} u_\mu u_\nu \delta^4[\mathbf{x} - \mathbf{z}(\tau)]$$

- Some Waveforms:



Circular orbits Orbits with $e = 0.188$ Zoom-Whirl orbits

Future Work

- Validate the Numerical Code for computations in the Lorentz gauge.

- Construct the necessary infrastructure for the computation of self-forces.

- The technology for computations in the case of a non-rotating SMBH are in place. This technology should be transfer to the case of a rotating (Kerr) SMBH, which is the case astrophysically relevant.

References

- CFS et al, CQG **23**, 251 (2006)
- CFS and P. Laguna, PRD **73**, 044028 (2006)